

# Crashworthiness Analysis and Morphology of Hybrid Hollow Tubes Reinforced by Aluminum Mesh with Hybrid Woven Fibre Composites (Basalt, Jute, Hemp, Banana, Bamboo) Using Roll-Wrapping Technique

Padmanabhan Rengaiyah Govindarajan,<sup>a,b,\*</sup> Rajesh Shanmugavel,<sup>c</sup> Sivasubramanian Palanisamy,<sup>d,\*</sup> Tabrej Khan,<sup>e</sup> Harri Junaedi,<sup>e</sup> Ajay Kumar,<sup>f</sup> and Tamer A. Sebaey<sup>e,g</sup>

This study investigated the mechanical performance of hybrid tubes made via roll-wrapping and enhanced with an aluminum mesh and epoxy matrix (AL-DMEM). The specimens included Basalt + Jute (BJAJB), Basalt + Bamboo (BBmABmB), Basalt + Banana (BBaABaB), Basalt + Hemp (BHABH), and Basalt (BAB). The BBmABmB specimen showed the best mechanical properties with the highest peak crushing force, specific energy absorption, mean crushing force, and total energy absorption. The AL-DMEM integration improved load-bearing capacity and energy absorption, reducing matrix cracking and fiber breakage. Scanning electron microscopy and energy-dispersive X-ray analysis highlighted BBmABmB's robust reinforcement. Its superior structural integrity and aluminum content make it suitable for applications requiring high structural integrity, such as micromobility vehicles, highlighting the potential of AL-DMEM-reinforced composites in advanced engineering applications.

DOI: 10.15376/biores.19.3.6584-6604

**Keywords:** Hollow structural tubes; Polymer composites; Basalt; Woven fibre; Aluminum mesh; Roll-wrapping; Energy absorption; Crushing force

**Contact information:** a: Department of Automobile Engineering, Kalasalingam Academy of Research and Education, Krishnankoil, 626126, Tamil Nadu, India; b: Department of Mechanical Engineering, Arasu Engineering College, Kumbakonam, 612501, Tamil Nadu, India; c: Department of Mechanical Engineering, Kalasalingam Academy of Research and Education, Krishnankoil, 626126, Tamil Nadu, India; d: Department of Mechanical Engineering, PTR College of Engineering and Technology, Austinpatti, Madurai, 625008, Tamil Nadu, India; e: Department of Engineering and Management, College of Engineering, Prince Sultan University, Riyadh, 11586, Saudi Arabia; f: Department of Mechanical Engineering, School of Engineering and Technology, JECRC University, Jaipur, India; g: Department of Mechanical Design and Production Engineering, Faculty of Engineering, Zagazig University, Zagazig 44519, Sharkia, Egypt; \*Corresponding authors: padhu003@gmail.com; sivaresearch948@gmail.com

## INTRODUCTION

In the structural crashworthiness segment of the composite material industry, hybridising fibre composites for energy absorption tube applications has gained attention. Chairman *et al.* (2020), highlighted the unique characteristics of basalt fibres, pointing out that they react non-toxically with water or air and do not burn when they chemically encounter other substances. Because of this, they are safe for human health and the environment. Persico *et al.* (2022), has assessed that the basalt fibres have been highlighted in a number of studies as a promising new reinforcing material for fibre-reinforced polymer (FRP) composites (Chairman *et al.* 2020; Almeshaal *et al.* 2022; Palanisamy *et al.* 2022; Persico *et al.* 2022). However, the respiratory safety of basalt fibers must be carefully

considered. Historically, asbestos fibers were highly acclaimed for their lack of flammability, favorable aspect ratio, and strength. Over time, they were condemned due to their severe health hazards, particularly respiratory diseases such as asbestosis, lung cancer, and mesothelioma (Stayner *et al.* 1996; LaDou 2004). This historical context necessitates a thorough investigation into the potential health risks associated with basalt fibers. Recent studies indicate that basalt fibers, unlike asbestos, do not pose a significant health risk when proper handling procedures are followed. Research by Adejuyigbe *et al.* (2019) and Horrocks *et al.* (2020) suggests that basalt fibers have a lower biopersistence in the lungs and do not induce the same level of chronic inflammation and fibrosis as asbestos fibers. Additionally, the International Agency for Research on Cancer (IARC) classifies basalt fibers as Group 3, “not classifiable as to their carcinogenicity to humans,” due to insufficient evidence (IARC, 2018). Despite these findings, it is crucial to continue monitoring and evaluating the long-term health impacts of basalt fiber exposure. Implementing safety measures during manufacturing and application processes can further mitigate potential risks. Proper ventilation, protective equipment, and adherence to occupational safety guidelines are essential to ensure the safe use of basalt fibers in various industries.

The potential for energy absorption of laminated composite materials—which are widely utilised in industries for their superior strength-to-weight ratio, affordability, and corrosion resistance—was investigated by Gowid *et al.* (2020). Due to the thin walls of the study objects, there is a strong probability of buckling rather than classical compression failure. This research employs a design strategy with higher-modulus layers on the outside and bulkier layers in the interior to resist buckling. The high-modulus outer layers provide increased stiffness and strength, preventing local buckling, while the bulkier interior layers enhance energy absorption and structural stability. This study tested the strength and energy-absorbing capacity of materials by examining the impacts of sandwich laminates composed of woven fibres and fibre steel inside PVC polymer tubes (Gowid *et al.* 2020). Supian *et al.* (2018) assessed the impact of hybridisation on energy absorption characteristics and crashworthiness behaviours in various composite types, including metal/synthetic fibre, synthetic/synthetic fibre, and natural/synthetic fibre composites (Supian *et al.* 2018; Karuppiyah *et al.* 2022). In the current work, bamboo fibre woven as cloth was used to manufacture a polymer composite through and lay process, which includes the application of uniform pressure using rollers to impregnate the fibres with the adhesive resin. Veeresh Kumar *et al.* (2021) reported that natural fibre provides both decreased density and cost savings in comparison with glass fibres. However, natural fibre resistance is not as good as glass, the specific characteristics are similar (Kumar *et al.* 2021b; Palaniappan *et al.* 2024). Through combining previous studies and considering the possibility of creating new hybrid composite fibre materials, especially from natural/synthetic fiber-reinforced composites, this review seeks to offer guidance for future research in high-performance energy absorption tube applications (Lv *et al.* 2019; Kurien *et al.* 2023). Aluminium wire meshes were used by Sadoun *et al.* (2021), to increase the epoxy/E-glass fibre combination’s durability. The researchers examined the effects of substituting some glass fibre layers with Al wire meshes inserted throughout the specimen’s thickness using a variety of tests, such as tensile, bending, and hardness evaluations, on the material's mechanical properties (Sadoun *et al.* 2021; Palanisamy *et al.* 2023a). According to Padmanabhan *et al.* (2022), there are no possible gaps between reinforcing metal layers during the lay-up process. A single piece of aluminium perforated mesh was carefully cut and rolled for each hybrid tube (Padmanabhan *et al.* 2022).

Remarkably, this method improved the hybrid tubes bonding capabilities, which may increase their chemical combination between metal and hybrid fibres as laminates. Better structural performance in a variety of applications was demonstrated by the integrated metal sheet, which leads to more stable crushing deformation (Mirzamohammadi *et al.* 2023).

In quasi-static studies, composite tubes made of fiber-reinforced thermoset resin bases were investigated (Ma *et al.* 2021). Abu Bakar *et al.* (2020), assessed the structural performance of same composite materials as above-mentioned with particular attention to fracture propagation and collapse modes (Bakar *et al.* 2020). In place of traditional metal sheet and concrete tubes, these tubes provide a strong, lightweight, and corrosion-resistant construction (Ma *et al.* 2021). Zhang *et al.* (2018) examined the mechanical properties and crashworthiness of composite tubes constructed from various resin-based materials. According to Alshahrani *et al.* (2023), basalt fibre can be added to jute fibre composites to reduce weight and cost of the vehicle without sacrificing strength and rigidity. An epoxy matrix was mixed with woven textiles consisting of jute and basalt fibers to create hybrid composite laminates (Sivagurunathan *et al.* 2018; Alshahrani *et al.* 2023).

Vinod *et al.* (2022) reported their study incorporates a wide variety of materials with different compositions and physical properties, as specified in Table 1a, fibres including jute, banana, hemp, and bamboo have different amounts of lignin, hemicellulose, and cellulose, as well as various moisture levels and densities (Vinod *et al.* 2022; Sumesh *et al.* 2023). Their densities range from 1.3 g/cm<sup>3</sup> to 0.5 g/cm<sup>3</sup>, and their surface densities range from 250 to 350 g/m<sup>2</sup>. Basalt has a density of 2.8 g/cm<sup>3</sup> and a thickness that ranges between 0.6 and 0.8 mm. The AL-DMEM 6061 alloy from Table 1b, primarily consisting of aluminium (Al) and containing elements, such as copper (Cu), magnesium (Mg), zinc (Zn), iron (Fe), chromium (Cr), manganese (Mn), and silicon (Si), in mesh form, enhances the mechanical strength of hybrid fibre metal laminates (HWFMLs) (Mohd Bakhori *et al.* 2022).

The present study investigated the crashworthiness of basalt/natural woven fibre polymer laminates made by roll-wrapping and hollow structural tubes reinforced with aluminium (AL-DMEM). Axial compression, radial compression, and transverse flexural analysis are three testing techniques used to assess the mechanical characteristics and structural performance of the hybrid composite tubes, as mentioned in another study (Mache *et al.* 2020). Test procedures that followed ASTM guidelines were applied to specimens including BJAJB, BBmABmB, BBaABaB, BHAHB, and BAB, amongst others, to evaluate their energy absorption properties, load-bearing capabilities, and crashworthiness behaviours (Mirzamohammadi *et al.* 2022). Furthermore, the integration of AL-DMEM and basalt/natural woven fibre polymer laminates is intended to improve the composite tubes' crash resistance and structural integrity. This may increase the range of industries in which these materials can be used, as they are lightweight, corrosion-resistant, and highly durable materials that can be used for structural protection and impact mitigation.

**Table 1a.** Chemical Composition with Specific Properties of HFML (Mohd Bakhori *et al.* 2022)

Materials	Lignin (wt%)	Hemi-cellulose (wt%)	Cellulose (wt%)	Moisture (wt%)	Density (g/cm <sup>3</sup> )	Thickness (mm)	Surface Density (g/m <sup>2</sup> )	Type
Jute	16	14	65	13	1.3	0.7	300	Woven
banana	11	27	44	16	1.3	0.7	300	Woven
hemp	9	23	67	10	1.4	0.8	300	Woven
bamboo	27	26	46	11	0.5	0.6	250	Woven
basalt	-	-	-	-	2.8	0.8	350	Woven
AL-DMEM 6061	-	-	-	-	1.8	0.9	650	mesh

**Table 1b.** Chemical Composition AL-DMEM 6061

AL-DMEM 6061	Aluminium (Al)	Copper (Cu)	Magnesium (Mg)	Zinc (Zn)	Iron (Fe)	Chromium (Cr)	Manganese (Mn)	Silicon (Si)
in %	95.9% - 98.7%	0.14% - 0.5%	0.8% - 1.2%	0.25% max	0.7% max	0.03% - 0.35%	0.15% max	0.4% - 0.8%

## EXPERIMENTAL

### Materials and Fabrication Methods

The primary objective of this research was to develop hybrid fiber metal laminates (HWFMLs) that meet specific performance criteria and quality standards. The goal was to create robust, durable composites with plant-based fibers that exhibit superior mechanical properties, such as high tensile strength, excellent energy absorption, and enhanced structural integrity. The inclusion of fibers like hemp, banana, bamboo, and jute aims to leverage their benefits while ensuring the composites perform optimally under various mechanical stresses. This approach seeks to advance composite material technology for high-performance applications in industries including automotive, aerospace, and construction. This HWFMLs, focus on their design, characterisation, and crashworthiness testing. These laminates use natural woven fibres (NWFs), such as hemp, banana, bamboo, and jute, as reinforcement materials along with commercial-grade aluminium 6061 alloy mesh (AL-DMEM) in an effort to create robust, long-lasting composite structures appropriate for a variety of applications (Alkbir *et al.* 2016). Basalt is a synthetic woven fibre that was purchased from Go Green Products Private Limited, Chennai, India and used as a surface material for laminates. It is necessary to appropriately mix the standard epoxy resin (LY 556) and hardener (HY 951) for additions, as they are defined according to their compatibility and bonding effectiveness (Padmanabhan *et al.* 2024). The materials used in the composite production process were supplied by the LMP R&D facility located in Erode, Tamilnadu, India.

Surface modification techniques are used to improve the interaction between the NWFs and the epoxy matrix (Palanisamy *et al.* 2023b). These techniques include an etching process that involves immersing an alkaline sodium hydroxide (NaOH) solution and washing the resultant material with distilled water (Sadoun *et al.* 2021). When plant-based fiber material is treated with NaOH, one of the most immediate and important effects

is the dissolution of some monomeric extractives, such as fatty acids. This is important because such monomers can impede the spreading of adhesives and act as a weak boundary layer, thereby hurting adhesion at interfaces. Another benefit shown in studies of NaOH treatment is that the fiber surfaces become rough due to the dissolution of wood extractives, as well as possibly silica and/or some lignin, depending on the concentration, temperature, and time of treatment. A rougher surface will have a higher area of contact with an adhesive, and mechanical interlocking can develop. Figure 1 shows that the hydrophilicity of the fibre surfaces was improved by this treatment, which makes mechanical interlocking and ideal bonding with the epoxy matrix easier. Furthermore, to attain standardization, the commercial-grade aluminium 6061 alloy mesh (Al-DMEM) was polished to have certain dimensions that are essential for strong interfacial adhesion with the epoxy matrix: 2 mm short way diamond (SWD), 4 mm long way diamond (LWD), and 0.9 mm in thickness.

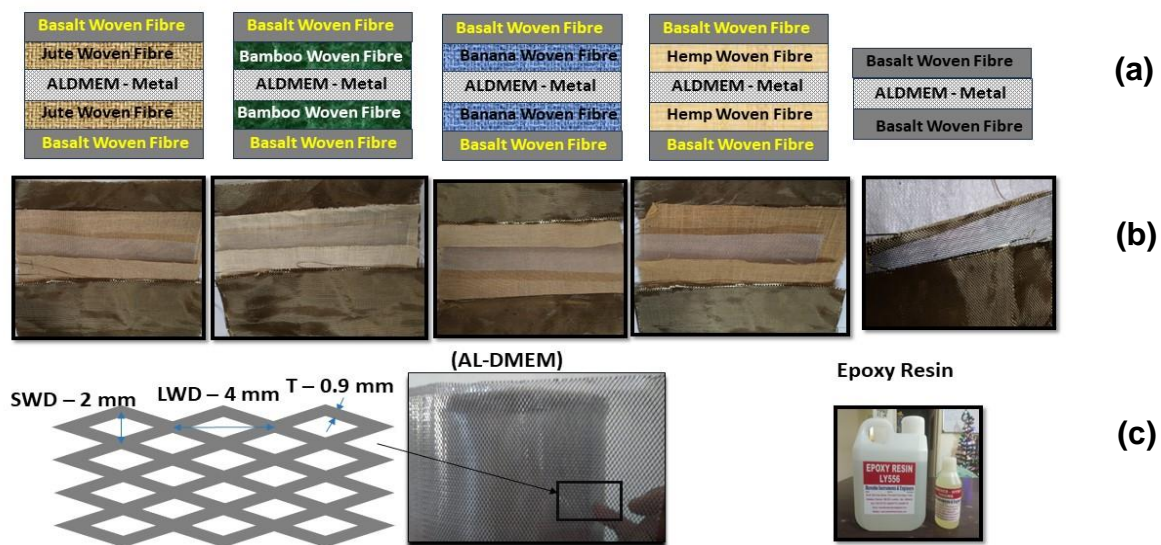


**Fig. 1.** Materials in HHS Tube: a) Orientation of HHS Tube, b) Stacking sequence of AL-DMEM in HWFL, and c) AL-DMEM with dimension and bonding agent

### Hollow Hybrid Structural (HHS) Tube Production

Roll-wrapping was utilised throughout the production phase to manufacture FRP tubes that consist of Al-DMEM mesh and resin-impregnated NWFs. From Fig. 2, enveloping layers of fibre reinforcement around a 32 mm-diameter cylinder mandrel ensures fibre distribution is uniform along the length of the tube (Padmanabhan *et al.* 2022). The HHS tube specimens that come from the combination of Al-strength DMEM's and FRP's flexibility provide enhanced crashworthiness and mechanical qualities. Following consolidation, which guarantees close contact between the fibre and resin and eliminates air bubbles, curing is performed to activate the resin matrix and produce a solid composite structure. After curing, finishing operations were applied to FRP tubes reinforced with HHS cores to achieve the necessary dimensions and surface quality.

Additionally, a range of material combinations were examined to evaluate their efficacy in HWFMLs. Five distinct combinations of NWFs, Al-DMEM mesh, and resin matrix were investigated, each with a unique layout. In the fabrication process of HWFMLs, tube layering largely influences mechanical properties and crashworthiness (Ma *et al.* 2022). From Table 2, five samples, BJALJB, BBmALBmB, BBaALBaB,

BHALHB, and BALB, of different material combinations for enhanced performance are listed. Sample BJALJB incorporated Al-DMEM mesh, jute, and basalt woven fabric layers, aiming to leverage tensile strength and interfacial adhesion. Similarly, BBmALBmB utilized bamboo, known for flexibility, with basalt and Al-DMEM layers for strength. BBaALBaB introduces impact-resistant banana fibers between Al-DMEM and basalt layers. BHALHB integrates hemp for enhanced structural integrity with Al-DMEM and basalt layers by the size of HHS tube specimens are  $450 \times 35 \times 3 \text{ mm}^3$ .

**Table 2.** Hybrid Tube Specimens and Fiber Layers

S. No.	Material Combination	Sample Code	Inner Layer	Middle Layer	Outer Layer	Resin
1.	Basalt + Jute + ALDMEM + Jute + Basalt	BJALJB	ALDMEM mesh – 1 layer	Jute Woven	Basalt Woven	Epoxy
2.	Basalt + Bamboo + ALDMEM + Bamboo + Basalt	BBmALBmB	ALDMEM mesh – 1 layer	Bamboo Woven	Basalt Woven	Epoxy
3.	Basalt + Banana + ALDMEM + Banana + Basalt	BBaALBaB	ALDMEM mesh – 1 layer	Banana Woven	Basalt Woven	Epoxy
4.	Basalt + Hemp + ALDMEM + Hemp + Basalt	BHALHB	ALDMEM mesh – 1 layer	Hemp Woven	Basalt Woven	Epoxy
5.	Basalt + ALDMEM + Basalt	BALB	ALDMEM mesh – 1 layer	-	Basalt Woven	Epoxy

A comprehensive crashworthiness analysis employs axial compression, three-point flexural, and radial compression tests to assess the energy absorption capacity and structural integrity of HWFMLs, as mentioned in Fig. 2 (Fan *et al.* 2021). The purpose of this methodical approach is to promote the comprehension and utilisation of hybrid composite materials in the field of structural engineering, with a particular focus on improving their performance and crashworthiness under the challenging conditions. In the aerospace, automotive, marine, and construction sectors, among others, the roll wrapping method is utilised to make lightweight, long-lasting components with individualised mechanical properties, in addition to providing manufacturing simplicity and design flexibility.

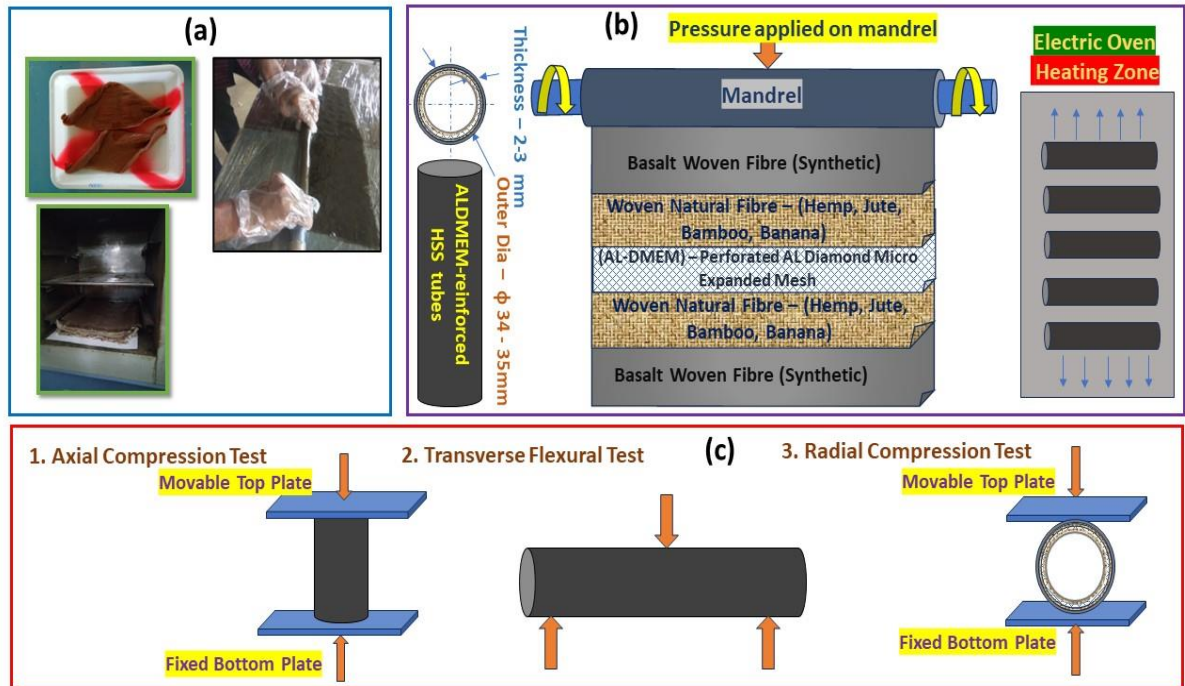


**Fig. 2.** Graphical abstract of HHS composite - a) Natural fibre chemical treatment, b) Roll wrapping method as fabrication technique, and c) Crashworthiness analysis tests

Overall, this work's specific methodology ensures optimal component adhesion, which further improves the mechanical properties and crash resistance of HWFMLs (Kumar *et al.* 2021a). The goal of this research is to significantly advance the development of high-performance composite materials suitable for a broad range of commercial applications through the integration of innovative production techniques, comprehensive material characterization, and meticulous testing procedures.

## Testing of Materials under Applied Load

### *Axial compression test*

The compressive strength of the produced tubes was assessed by an axial compression test following the ASTM D5449 (2018) standard and the methodology described by Heckadka *et al.* (2018) to ensure analytical rigidity. The standardised process entailed applying compressive stresses on tubes made of aluminium and carbon fibre-reinforced polymer (CFRP) at a constant pace of 5 mm/min under room temperature conditions (Ma *et al.* 2021). The tubes selected for the compressive testing were customised to match the materials utilised and showed distinct dimensional characteristics (Rouzegar *et al.* 2018). Figure 3a illustrates that the tubes classified as BJAJB, BBmABmB, BBaABaB, BHAHB, and BAB had initial dimensions of 60 mm in length, 3 to 3.5 mm in thickness, and a diameter ranging from 34 to 35 mm before testing. Fractures mostly occurred at the margins during the axial compression test because of fibre peeling and deformation of the ALMEM. The failure mode was evident in all specimens, emphasising the crucial weak areas in the materials when subjected to compressive pressure (Ding *et al.* 2018). According to Sivagurunathan *et al.* (2018), the compaction region is the area that comes after the post-crushing phase in axial compression testing. The buildup of debris and the total compression of the tube mass cause a non-linear and sudden increase in load during this period (Sivagurunathan *et al.* 2018). The test yielded useful insights into the

compressive strength and behavioural responses of the tubes, despite certain failures in specific areas. The results greatly enhance comprehension of the structural performance of the tubes and aid in making engineering decisions related to material selection and structural design.

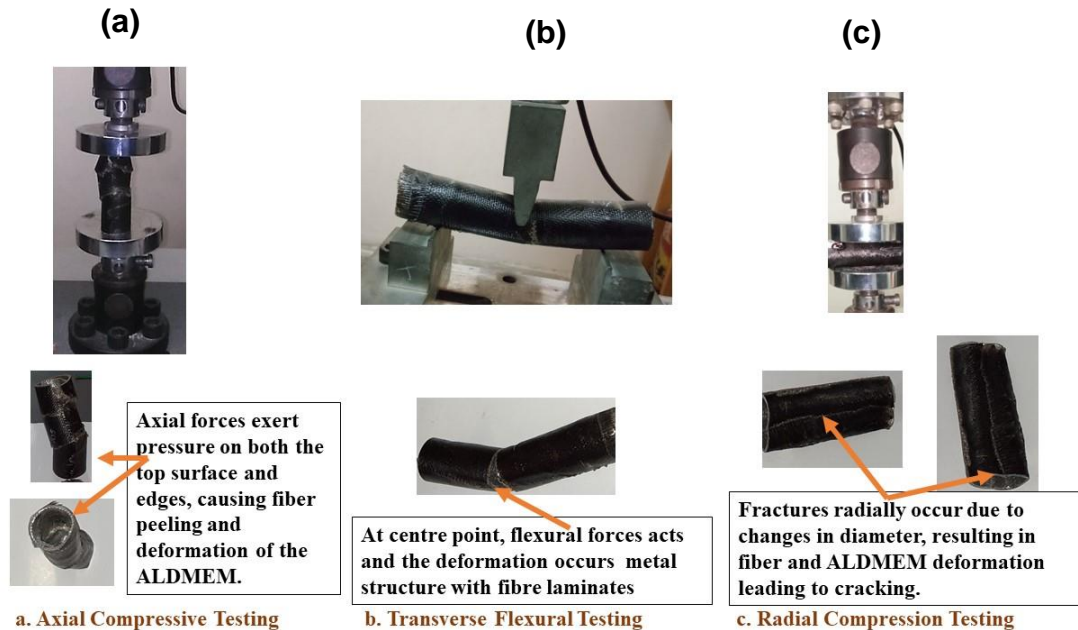


**Fig. 3.** Specimens with deformation analysis: a) Axial compression, b) Transverse flexural, and c) Radial compression testing of hybrid composite tubes reinforced with aluminum mesh and epoxy matrix (ALDMEM) (Govindarajan *et al.* 2024).

#### *Transverse flexural test*

A three-point flexural test, conducted in accordance with ASTM D790 (2010) guidelines, was used to determine the maximum fracture force and flexural strength of HHS tube specimens (Ma *et al.* 2021). A controlled force application was applied to each specimen, namely BJAJB, BBmABmB, BBaABaB, BHAHB, and BAB, at a rate of 5 mm/min until the outer surface ruptured (Prasath *et al.* 2020). A comprehensive assessment of mechanical qualities was ensured by precisely identifying flexural failure by the analysis of force-displacement curves up to their peak value. Figure 3b shows that the specimens initially had measurements in accordance with ASTM D790 (2010) standards and the methodology described by Lv *et al.* (2019) a length of 300 mm, a thickness between 3 and 3.5 mm, and a diameter ranging from 34 to 35 mm. To ensure testing accuracy and consistency, supports were positioned 200 mm apart, in accordance with ASTM specifications (Dhaliwal and Newaz 2016). Flexural strength for each specimen was calculated using test results and applied maximum force, which gave important information about mechanical characteristics and application compatibility (Bahari-Sambran *et al.* 2020). Comprehensive analysis and interpretation of tube performance parameters depend on the consistent adherence to testing standards and the documenting of specimen specifications, which provide precise and reliable testing results.

#### *Radial compression test*

This test was performed to assess the structural integrity and radial compressive strength of the manufactured tubes, which included different fibre compositions and

ALDMEM mesh. The testing was conducted in accordance with the ASTM D2412 (2016) standard and the methodology described by Supian *et al.* (2020). The specimens consist of HHS tubes with varying fibre compositions named BJAJB, BBmABmB, BBaABaB, BHAHB, and BAB as specimens. Figure 3c shows that the tubes were placed on the testing apparatus and exposed to compressive forces in the radial direction at a regulated speed (Bellini *et al.* 2022). Energy Absorption (EA), Specific Energy Absorption (SEA), Mean Crush Force (MCF), Crush Force Efficiency (CFE), and Peak Crushing Force (PCF) were also measured and analysed to understand the energy absorption capacities and structural performance during radial compression (Ma *et al.* 2021). Fracture patterns, force-displacement curves, fibre content, and ALDMEM mesh content were recorded to correlate with mechanical responses. This testing method provides important data for choosing materials and making structural design choices, particularly in situations where radial compressive loads are important factors.

Crashworthiness testing, including axial, transverse, and radial compression, were carried out at the “LMP Research and Development Lab” situated in Erode. The tests utilised a servo-hydraulic Computerised Universal Testing Machine (KIC-2-1000C; Kalpak Instruments and Controls Pvt, Ltd., India) with interchangeable load cells and a 25 KN capacity. The configuration established by “LMP Research and Development Lab” ensured precise assessments of the tubes’ structural integrity under varying loading circumstances.

### Crashworthiness Indicators

In the intricate process of crushing, the thin-walled structures can demonstrate their ability to absorb the substantial impact energy through intrinsic plastic deformation efficiently. This design concept is supported by the results in Figs. 4 and 6. Figure 4 shows that the high-modulus outer layers maintained structural integrity and prevented buckling under axial load. Figure 6 highlights the improved performance of the composite tubes with this layered design, demonstrating their suitability for high-performance applications in automotive, aerospace, and construction industries. This inherent characteristic significantly mitigates the impact load generated during collisions. The judicious selection of crash performance evaluation indicators proves paramount for a thorough assessment of thin-walled structures’ crashworthiness (Zhu *et al.* 2019). The commonly employed indicators encompass the total energy absorption, specific energy absorption (SEA), initial peak load, average crushing load, and crushing force efficiency. These indicators can capture and define various aspects of the structure's crash performance meticulously, providing a comprehensive understanding of its ability to dissipate energy and to withstand impact forces.

Indicators of energy absorption are essential for determining a structure’s crashworthiness, especially in situations where axial crushing occurs (Alhyari and Newaz 2021). Energy Absorption (EA), which measures the overall energy lost during crushing, is one basic indicator. The EA can be computed mathematically as the integral of the crushing force ( $F$ ) relative to the displacement ( $\delta$ ), which can be expressed by the following formula:

$$EA = \int Fd\delta \quad (1)$$

A normalised measurement is provided by SEA, which takes the absorbed energy into account in relation to the structure's total mass ( $m$ ). It helps in the comparison of various energy absorbers and is calculated as follows (Yang *et al.* 2020):

$$SEA = \frac{\int Fd\delta}{m} \quad (2)$$

The average force used during crushing is revealed by the Mean Crush Force (MCF). It is calculated by dividing the crushing distance ( $\delta$ ) by the energy absorbed (EA), and is stated as follows:

$$MCF = \frac{SEA}{\delta} \quad (3)$$

The Crush Force Efficiency (CFE) measures how well energy is absorbed in relation to the peak crushing force ( $F_p$ ). The CFE is described by the following Eq. 4, which takes the ratio of the mean crushing force ( $F_m$ ) to the peak crushing force ( $F_p$ ):

$$CFE = \frac{F_m}{F_p} \quad (4)$$

In an ideal scenario, optimizing all aspects of energy absorption would yield a CFE value of 100%. The comprehensive suite of these indicators offers a detailed insight into the structural performance and the effectiveness of energy absorption devices in mitigating impact forces during compression.

### SEM with EDX Analysis

The investigation of hybrid tube specimens BJALJB, BBmALBmB, BBaALBaB, BHALHB, and BALB, involved a comprehensive analysis utilizing scanning electron microscopy (SEM, EVO18, Carl Zeiss) combined with energy-dispersive X-ray spectroscopy (EDX, Quantax 200 with X Flash® 6130). The SEM-EDX analysis provided detailed insights into the elemental composition and fracture mechanisms of each specimen.

**Table 3.** Elemental Composition and Percentage of Hybrid Tube Specimens

Specimen	Carbon (C) Weight %	Carbon (C) Atomic %	Oxygen (O) Weight %	Oxygen (O) Atomic %	Aluminum (Al) Weight %	Aluminum (Al) Atomic %	Silicon (Si) Weight %	Silicon (Si) Atomic %	Calcium (Ca) Weight %	Calcium (Ca) Atomic %	Iron (Fe) Weight %	Iron (Fe) Atomic %
BJALJB	54.50%	71.90%	11.20%	10.10%	33.40%	19.53%	0.32%	0.28%	0.35%	0.17%	0.82%	0.26%
BBmALBmB	57.70%	71.80%	18.90%	15.20%	23.60%	11.90%	1.35%	0.80%	0.30%	0.20%	0.70%	0.30%
BBaALBaB	66.50%	75.60%	21.40%	18.50%	12.10%	6.20%	0.12%	0.10%	-	-	-	-
BHALHB	57.20%	68.00%	28.00%	25.00%	1.30%	0.80%	0.80%	0.50%	4.70%	2.50%	4.30%	2.20%
BALB	62.30%	69.20%	35.90%	29.90%	0.60%	0.30%	0.40%	0.20%	0.20%	0.10%	-	-

These elements were found at varying weights and atomic percentages, indicative of the composite's composition and potential failure modes, such as jute fibre peeling out from bonding, and void content occurs.

Similarly, specimen BBmALBmB exhibited distinctive elemental compositions, with notable proportions of (C) detected at a 57.7% and an 71.8%, (O) at 18.9% and 15.2%, (Al) at 23.6% and 11.9%, (Si) at 1.35% and 0.8%, (K) at 0.3% and 0.2%, (Ca) at 0.7% and 0.3%, and (Fe) at 0.8% and 0.3%. These findings, coupled with SEM imaging, allowed for a deeper understanding of the fracture mechanisms in bamboo fibre and material behavior as discontinued by testing. Specimen BBaALBaB displayed a different elemental distribution, highlighting the presence of (C) exhibited 66.5% and 75.6%, (O) at 21.4%

and 18.5%, (Al) at 12.1% and 6.2%, and (Si) at 0.12% and 0.0%. These findings provided valuable insights into the composition and potential failure mechanisms of the banana woven crushes and peel out from laminate. In specimen BHALHB, the presence of (C) was detected at 57.2% and 68.0%, (O) at 28.0% and 25.0%, (Na) at 1.3% and 0.8%, (Mg) at 0.8% and 0.5%, (Al) at 4.7% and 2.5%, (Si) at 4.3% and 2.2%, (K) at 0.4% and 0.2%, (Ca) at 0.9% and 0.3%, and (Fe) at 2.4% and 0.6%. These elemental compositions, along with SEM imaging, aided in identifying deformation by hemp fibre pull out and failure modes as matrix deformation within the laminate. Lastly, specimen BALB exhibited distinct elemental proportions, (C) exhibited at 62.3% and 69.2%, (O) at 35.9% and 29.9%, (Mg) at 0.6% and 0.3%, (Al) at 0.6% and 0.3%, (Si) at 0.4% and 0.2%, and (Ca) at 0.2% and 0.1% detected. The SEM-EDX analysis provided valuable information regarding the material's composition and potential failure mechanisms.

## RESULTS AND DISCUSSION

The mechanical characteristics and performance of the five specimens—BJAJB, BBmABmB, BBaABaB, BHAHB, and BAB—are thoroughly examined in this section. The preliminary stages of testing provide information about the specimens' crashworthiness and strength by identifying differences in the specimens' mean load, peak load, and SEA.

### Axial Compressive Analysis

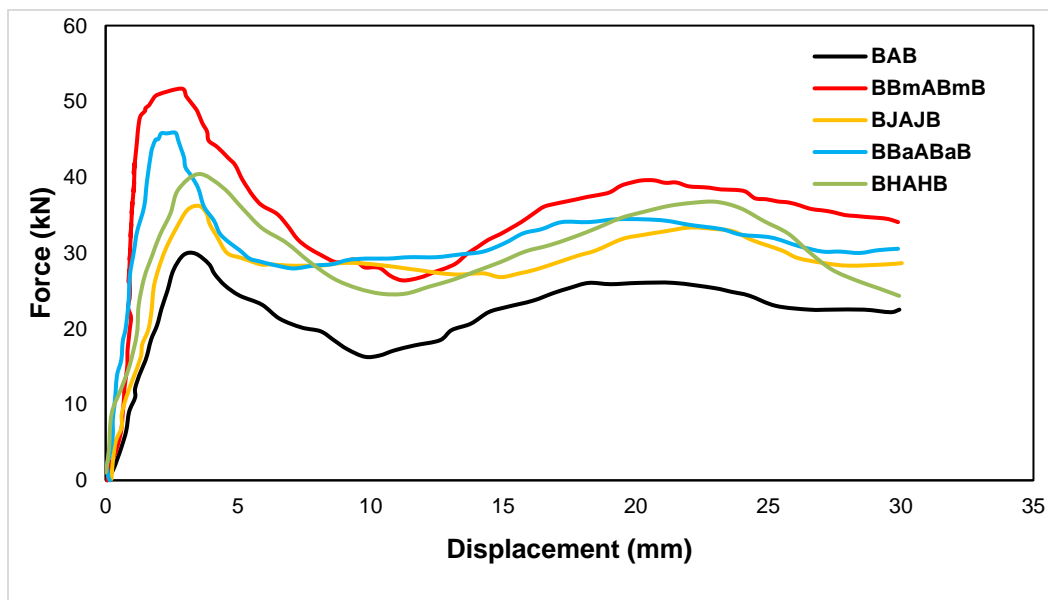


**Fig. 4.** Force-displacement curve for all 5 specimens subjected to axial compressive analysis

The axial compressive behaviour of hybrid tube specimens including BJAJB, BBmABmB, BBaABaB, BHAHB, and BAB offers important insights into their mechanical response to compression. Table 3 and Fig. 4 show that the BBmABmB had the highest PCF of 51.687 kN, showing a notable increase of almost 73% compared to BAB, which had the lowest PCF of 29.916 kN. BBaABaB and BHAHB showed higher PCF

values than BAB, with increases of around 53% and 35% respectively. BJAJB had a PCF of 36.201 kN, showing a 17% improvement over BAB. BBmABmB exhibited the highest EA value of 973.67 J, representing a significant increase of almost 52% compared to BAB. BBaABaB and BHAHB showed enhancements of about 41% and 36%, respectively. BJAJB displayed an energy availability of 818.12 J, representing a 27% rise compared to BAB. BBmABmB had the highest MCF of 36.087 kN, which was about 74% better than BAB. BBaABaB and BHAHB also had higher MCF values than BAB, around 46% and 39% higher, respectively. BJAJB had an MCF of 27.821 kN, showing a 34% improvement over BAB. BBmABmB had the highest SEA at 13.186 J/g, which was about 39% better than BAB. BBaABaB and BHAHB showed improvements of around 29% and 20%, respectively. BJAJB had a SEA of 10.89 J/g, representing a 15% increase compared to BAB. BBmABmB had the greatest CFE rating, followed by BHAHB, BBaABaB, BJAJB, and BAB, indicating differences in their capacity to absorb and release energy while being compressed. BBmABmB had the lowest deflection of 2.859 mm, followed by BBaABaB, BHAHB, BJAJB, and BAB, showing differences in their structural stiffness and deformation when subjected to compressive pressure. The study highlights the significance of material composition and structure in influencing the compressive strength and energy absorption of hybrid tube structures. BBmABmB showed the best mechanical performance compared to other samples.

**Table 4.** Performance Parameters for HHS Tubes from Axial Compression Load Test

Specimens	PCF (kN)	EA (J)	MCF (kN)	SEA (J/g)	CFE	Deflection ( $\delta$ )
BJAJB	36.201	818.12	27.821	10.89	0.769	3.533
BBmABmB	51.687	973.67	36.087	13.186	0.699	2.859
BBaABaB	45.852	908.29	30.185	12.243	0.656	2.634
BHAHB	40.42	876.12	28.832	11.357	0.713	3.518
BAB	29.916	642.17	20.672	9.46	0.69	3.389

### Transverse Flexural Analysis

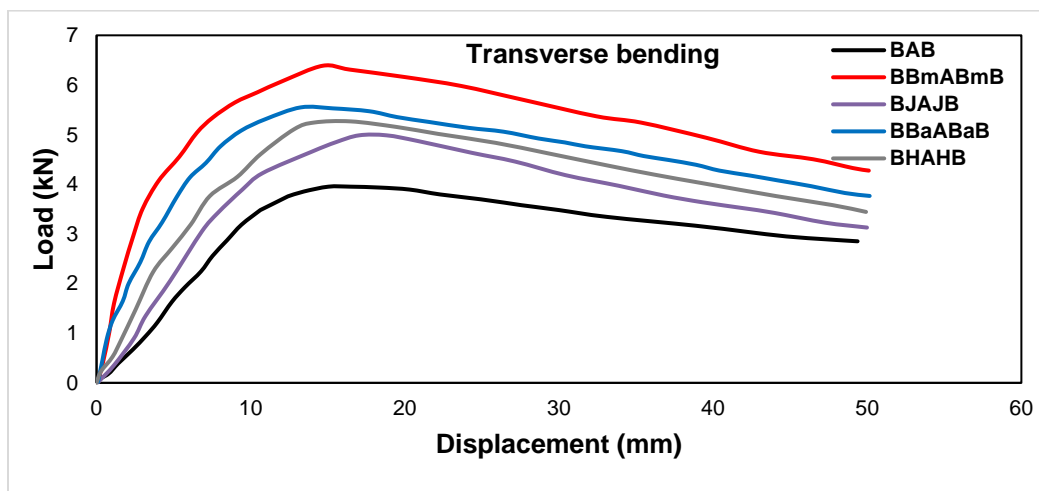


**Fig. 5.** Force-displacement curve for all 5 specimens subjected to transverse flexural analysis

Hybrid tube specimens BJAJB, BBmABmB, BBaABaB, BHAHB, and BAB were subjected to collision resistance trials to evaluate their transverse compression performance. Through meticulous analysis, the specimens were scrutinized to assess their deformation characteristics and collision resistance capabilities.

**Table 5.** Performance Parameters for HHS Tubes from Transverse Flexural Load Test

Specimens	PCF (kN)	EA (J)	MCF (kN)	SEA (J/g)	CFE	Deflection ( $\delta$ )
BJAJB	4.986	73.54	4.187	1.606	0.997	18.814
BBmABmB	6.387	93.77	5.981	2.636	1.313	14.669
BBaABaB	5.549	91.24	5.059	2.347	1.127	13.249
BHAHB	5.267	87.11	4.378	2.008	1.093	16.484
BAB	3.952	65.03	3.343	1.498	0.988	16.458

The results unveiled distinct force-displacement patterns, showcasing variations in strength and energy absorption among the specimens. Table 4 and Fig. 5 show that these results focused on the mechanical performance of hybrid tubes crafted *via* roll-wrapping and enhanced with an aluminium mesh and epoxy matrix (ALDMEM). Among 5 specimens, BBmABmB exhibited superior mechanical properties, surpassing BJAJB in peak force by over 28%. BBaABaB and BHAHB followed with improvements of 23% and 19%, respectively. BBmABmB also achieved the highest Specific Energy Absorption (SEA), with a 63% increase over BAB, while BBaABaB and BHAHB showed enhancements of 57% and 50%, respectively. Additionally, BBmABmB demonstrated the highest Mean Crushing Force (MCF), with a 79% increase over BAB, and its Energy Absorption (EA) was 44% higher. BBaABaB and BHAHB exhibited notable MCF improvements of 51% and 31%, and EA enhancements of 40% and 34%, respectively. These findings underscore the distinct performance characteristics of the hybrid tube specimens, highlighting the advantages of specific configuration in terms of force-displacement behavior and energy absorption capacities.

### Radial Compressive Analysis

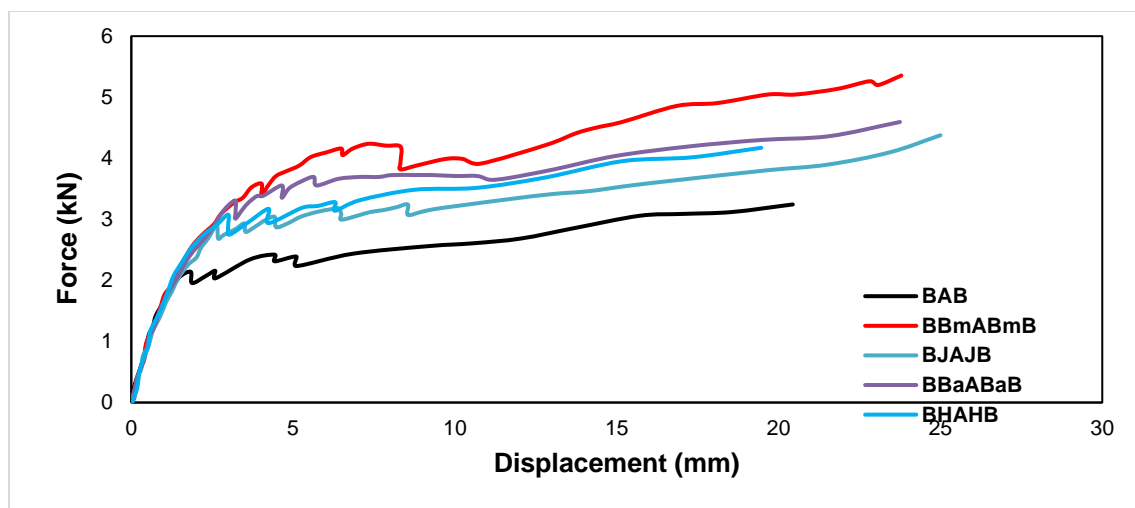


**Fig. 6.** Force-displacement curve for all 5 specimens subjected to radial compressive analysis

The investigation of hybrid tube specimens, such as BJAJB, BBmABmB, BBaABaB, BHAHB, and BAB, using radial compressive analysis offers valuable insights into their mechanical response to radial loading circumstances. From Table 5 and Fig. 6, BBmABmB showed a PCF of 4.237 kN. Among them, BBmABmB showed a Peak Crushing Force (PCF) around 75% higher than BAB, with BBaABaB and BHAHB showing increases of about 52% and 36%, respectively. BJAJB had a PCF approximately 34% higher than BAB. Regarding Energy Absorption (EA), BBmABmB exhibited an EA approximately 26% higher than BAB, with BBaABaB and BHAHB showing enhancements of about 16% and 7%, respectively. BJAJB had an EA about 5% higher than BAB. In terms of Mean Crushing Force (MCF), BBmABmB had the highest value, about 67% higher than BAB, while BBaABaB and BHAHB were approximately 53% and 38% higher, respectively. BJAJB showed an MCF around 30% higher than BAB. For Specific Energy Absorption (SEA), BBmABmB had a significant improvement of around 90% compared to BAB, with BBaABaB and BHAHB showing increases of about 76% and 44%, respectively. BJAJB had a SEA of 1.24 J/g, indicating a 27% increase over BAB. BBmABmB had the greatest CFE rating, followed by BHAHB, BBaABaB, BJAJB, and BAB, indicating differences in their capacity to absorb and release energy while being compressed. Regarding deflection ( $\delta$ ), BBmABmB had the lowest deflection of 7.335 mm, followed by BJAJB, BHAHB, BBaABaB, and BAB, showing differences in their structural stiffness and deformation response to radial loading. The integration of ALDMEM significantly enhanced the mechanical performance of these hybrid tubes. BBmABmB exhibited excellent load-bearing capacity and energy absorption, significantly reducing failure modes such as matrix cracking and fiber breakage. This enhancement is attributed to the improved stress distribution and interfacial integrity provided by ALDMEM. BBaABaB showed good structural performance with better energy absorption and load-bearing capabilities, attributed to reduced matrix cracking. BHAHB demonstrated enhanced load-bearing capacity due to decreased fiber breakage, offering better mechanical performance compared to traditional materials. Overall, the integration of ALDMEM in these hybrid tubes significantly improved their mechanical performance, making them highly suitable for applications requiring high structural integrity, such as micromobility vehicles. The outstanding properties of BBmABmB, in particular, underscore its potential for further optimization in advanced engineering applications.

**Table 6.** Performance Parameters for HHS Tubes from Radial Compression Load Test

Specimens	PCF (kN)	EA (J)	MCF (kN)	SEA (J/g)	CFE	Deflection ( $\delta$ )
BJAJB	3.244	71.84	3.12	1.24	0.62	6.295
BBmABmB	4.237	86.46	3.989	1.86	0.83	7.335
BBaABaB	3.694	79.15	3.647	1.72	0.74	5.635
BHAHB	3.281	73.47	3.313	1.41	0.71	6.295
BAB	2.421	68.42	2.391	0.98	0.58	4.428

## SEM with EDX Failure Modes

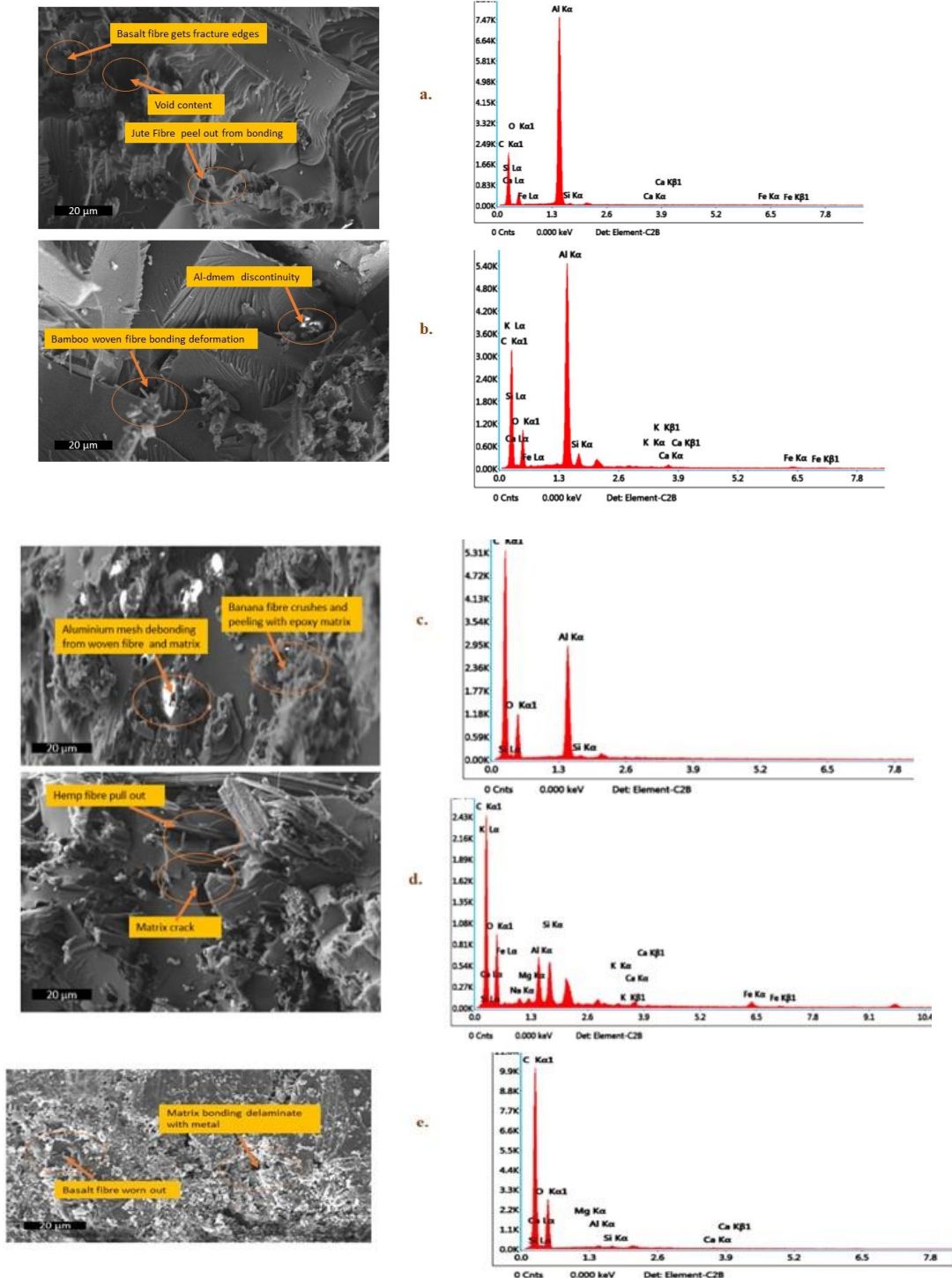


**Fig. 7.** SEM with EDX analysis of fracture specimens: a. BJALJB, b. BBmALBmB, c. BBaALBaB, d. BHALHB, and e. BALB

Figure 7 displays SEM images of hybrid polymer-metal reinforced laminates, revealing crucial failure modes through SEM analysis. The micrographs show regions where the metal and plant-based fibers are in close proximity, and the differences in

ductility had caused interfacial debonding and sliding. These images illustrate how the mechanical mismatch between the ductile metal and the relatively brittle plant-based fibers can lead to failure modes such as cracking and delamination. For instance, in Fig 7, micrographs reveal voids and gaps at the interface, suggesting that the sliding and separation occurred due to the disparate mechanical properties of the adjacent materials. This evidence supports the conclusion that enhancing the interfacial bonding and reducing the contrast in physical properties are crucial for improving the overall performance and reliability of the hybrid composites. The SEM-EDX analysis of the five hybrid tube specimens provided valuable insights into their elemental composition and fracture mechanisms. The specimen of BJALJB exhibited significant carbon content, suggesting robust fiber presence, yet was marred by fiber breakage and matrix cracking, indicating potential stress concentration and bonding issues. In contrast, the specimen BBmALBmB displayed high carbon and aluminium content, indicative of sturdy reinforcement, but was plagued by matrix cracking and metal deformation, signalling potential challenges under loading. The specimen BBaALBaB, with its distinct elemental composition and presence of delamination and surface fracture features, highlighted concerns regarding bonding integrity and fracture mechanics. Similarly, the specimen BHALHB, with its complex composition and interface integrity issues, underscored challenges in layer bonding and matrix reinforcement interaction. In addition, the specimen BALB, despite its simpler elemental composition, exhibited surface fracture features and microstructural defects, emphasizing the need for meticulous manufacturing and processing control. Overall, these findings underscore the importance of addressing bonding integrity, reinforcement distribution, and processing parameters to optimize the mechanical performance of hybrid laminates.

## CONCLUSIONS

1. Through crashworthiness analysis, BBmABmB was determined to be the highest-performing hybrid tube in all tests, demonstrating exceptional mechanical qualities. During the axial compression test, BBmABmB had the highest Peak Crushing Force (PCF) of 51.7 kN, Energy Absorption (EA) of 974 J, Mean Crushing Force (MCF) of 36.1 kN, and Specific Energy Absorption (SEA) of 13.2 J/g, outperforming other specimens by considerable margins.
2. Integrating ALDMEM mesh improved BBmABmB's performance by increasing its load-bearing capacity and energy absorption capabilities. BBmABmB showed the maximum performance in the transverse flexural test with a PCF of 4.24 kN, EA of 86.5 J, MCF of 3.99 kN, and SEA of 1.86 J/g. BBmABmB fared the best in the radial compression test, achieving a PCF of 4.24 kN, EA of 86.5 J, MCF of 3.99 kN, and SEA of 1.86 J/g compared to other specimens.
3. The remarkable mechanical qualities and integration of ALDMEM make it an ideal choice for micromobility and high-performance applications that need superior structural integrity and crash resistance.
4. In SEM-EDX analysis of hybrid tube specimens, BBmALBmB excelled with high carbon and aluminium content, indicating robust reinforcement. Though matrix cracking and metal deformation were noted, overall structural integrity appeared promising. This highlights BBmALBmB's potential for further refinement,

- underscoring the importance of addressing bonding integrity and processing parameters. ALDMEM mesh dramatically improved BBmABmB's mechanical characteristics. The hybrid tube outperformed samples without ALDMEM mesh in load-bearing and energy absorption. Improved bonding strength and interfacial integrity increased structural strength and crash resistance.
5. Analysis revealed that the hybrid tube structure's effective stress and strain distribution improved BBmABmB's performance. Fiber breakage and matrix cracking were decreased by the ALDMEM mesh, improving structural integrity and durability. This emphasizes the necessity for advanced bonding materials such as ALDMEM mesh to improve hybrid tube performance. BBmABmB's mechanical properties and ALDMEM integration make it the best micromobility alternative. Lightweight design, impact resistance, and durability provide rider safety and vehicle longevity in challenging urban environments. The ALDMEM-enhanced hybrid tube excels in structurally strong micromobility applications. BBmABmB outperformed all other specimens in axial and radial compression tests for mechanical strength and energy absorption. BBmABmB is the best hybrid tube for industrial applications because of its consistent performance across all parameters, exceeding other specimens that also provided improvements over standard materials. Hybrid tube technology's best mechanical performance and longevity is BBmABmB with ALDMEM integration. Its superior performance in all tests, ALDMEM integration, and failure process understanding make it the best choice for micromobility (E-Vehicle) panels and structural frames.

## ACKNOWLEDGMENTS

The authors express their gratitude to the Kalasalingam Academy of Research and Education organization for generously providing the fabrication and test facilities.

The authors would like to acknowledge the support of Prince Sultan University, Riyadh for paying the Article Processing Charge (APC) of this publication.

## Data Availability Statement

Data is available on request from the authors.

## Declaration of Conflicting Interests

The authors declared no potential conflicts of interest with respect to the research, authorship, and/or publication of this article.

## REFERENCES CITED

- Adejuyigbe, I. B., Paschal C. Chiadighikaobi, and Donatus A. Okpara. (2019). "Sustainability comparison for steel and basalt fiber reinforcement, landfills, leachate reservoirs and multi-functional structure," *Civil Engineering Journal* 5(1), 172-180. DOI: 10.28991/cej-2019-03091235
- Alhyari, O., and Newaz, G. (2021). "Energy absorption in carbon fiber composites with holes under quasi-static loading," *Journal of Carbon Research* 7(1), article 16. DOI:

10.3390/c7010016

- Alkbir, M. F. M., Sapuan, S. M., Nuraini, A. A., and Ishak, M. R. (2016). "Fibre properties and crashworthiness parameters of natural fibre-reinforced composite structure: A literature review," *Composite Structures* 148, 59-73. DOI: 10.1016/j.compstruct.2016.01.098
- Almehaal, M., Palanisamy, S., Murugesan, T. M., Palaniappan, M., and Santulli, C. (2022). "Physico-chemical characterization of *Grewia monticola* Sond (GMS) fibers for prospective application in biocomposites," *Journal of Natural Fibers* 19(17), 15276-15290. DOI: 10.1080/15440478.2022.2123076
- Alshahrani, H., Sebaey, T. A., Awd Allah, M. M., and Abd El-baky, M. A. (2023). "Jute-basalt reinforced epoxy hybrid composites for lightweight structural automotive applications," *Journal of Composite Materials* 57(7), 1315-1330. DOI: 10.1177/00219983231155013
- ASTM D2412 (2016). "Plastic pipe deflection testing," ASTM International, West Conshohocken, PA, USA.
- ASTM D5449 (2018). "Transverse compression fixture," ASTM International, West Conshohocken, PA, USA.
- ASTM D790 (2010). "Standard test methods for flexural properties of unreinforced and reinforced plastics and electrical insulating materials," ASTM International, West Conshohocken, PA, USA.
- Bahari-Sambran, F., Eslami-Farsani, R., and Arbab Chirani, S. (2020). "The flexural and impact behavior of the laminated aluminum-epoxy/basalt fibers composites containing nanoclay: An experimental investigation," *Journal of Sandwich Structures & Materials* 22(6), 1931-1951. DOI: 10.1177/1099636218792693
- Bakar, M. S. A., Salit, M. S., Yusoff, M. Z. M., Zainudin, E. S., and Ya, H. H. (2020). "The crashworthiness performance of stacking sequence on filament wound hybrid composite energy absorption tube subjected to quasi-static compression load," *Journal of Materials Research and Technology* 9(1), 654-666. DOI: 10.1016/j.jmrt.2019.11.006
- Bellini, C., Di Cocco, V., Iacoviello, F., and Mocanu, L. P. (2022). "Numerical modelling of fibre metal laminate flexural behaviour," *Material Design & Processing Communications* 2022, 1-8. DOI: 10.1155/2022/3401406
- Chairman, C. A., Thirumaran, B., Babu, S. P. K., and Ravichandran, M. (2020). "Two-body abrasive wear behavior of woven basalt fabric reinforced epoxy and polyester composites," *Materials Research Express* 7(3), article ID 35307. DOI: 10.1088/2053-1591/ab7de9
- Dhaliwal, G. S., and Newaz, G. M. (2016). "Experimental and numerical investigation of flexural behavior of carbon fiber reinforced aluminum laminates," *Journal of Reinforced Plastics and Composites* 35(12), 945-956. DOI: 10.1177/0731684416632606
- Ding, L., Liu, X., Wang, X., Huang, H., and Wu, Z. (2018). "Mechanical properties of pultruded basalt fiber-reinforced polymer tube under axial tension and compression," *Construction and Building Materials* 176, 629-637. DOI: 10.1016/j.conbuildmat.2018.05.036
- Fan, D., Qi-hua, M., Xue-hui, G., and Tianjun, Z. (2021). "Crashworthiness analysis of perforated metal/composite thin-walled structures under axial and oblique loading," *Polymer Composites* 42(4), 2019-2036. DOI: 10.1002/pc.25954
- Govindarajan, P. R., Shanmugavel, R., Palanisamy, S., Khan, T., and Ahmed, O. S.

- (2024). "Crash-worthiness analysis of hollow hybrid structural tube by aluminum with basalt-bamboo hybrid fiber laminates by roll wrapping method," *BioResources* 19(2), 3106-3120. DOI: 10.15376/biores.19.2.31063120
- Gowid, S., Mahdi, E., Renno, J., Sassi, S., Kharmanda, G., and Shokry, A. (2020). "Experimental investigation of the crashworthiness performance of fiber and fiber steel-reinforced composites tubes," *Composite Structures* 251, article ID 112655. DOI: 10.1016/j.compstruct.2020.112655
- Heckadka, S. S., Nayak, S. Y., Vishal, S. P., and Amin, N. M. (2018). "Evaluation of flexural and compressive strength of e glass/jute and e glass/banana hybrid epoxy hollow composite shafts," *Key Engineering Materials* 777, 438-445. DOI: 10.4028/www.scientific.net/kem.777.438
- Horrocks, A. R. (2020). "The potential for bio-sustainable organobromine-containing flame retardant formulations for textile applications—a review," *Polymers* 12(9), 2160. DOI: 10.3390/polym12092160
- International Agency for Research on Cancer (IARC). (2018). "Monographs on the evaluation of carcinogenic risks to humans, Volume 111," *Some Nanomaterials and Some Fibers*. [IARC website](https://monographs.iarc.fr/wp-content/uploads/2018/06/mono111.pdf)
- Karuppiyah, G., Kuttalam, K. C., Ayrilmis, N., Nagarajan, R., Devi, M. P. I., Palanisamy, S., and Santulli, C. (2022). "Tribological analysis of jute/coir polyester composites filled with eggshell powder (ESP) or nanoclay (NC) using grey rational method," *Fibers* 10(7), article 60. DOI: 10.3390/fib10070060
- Kumar, A. P., Maneiah, D., and Sankar, L. P. (2021a). "Improving the energy-absorbing properties of hybrid aluminum-composite tubes using nanofillers for crashworthiness applications," *Proceedings of the Institution of Mechanical Engineers, Part C: Journal of Mechanical Engineering Science* 235(8), 1443-1454. DOI: 10.1177/0954406220942267
- Kumar, G. B. V., Kishore, C. N., Kanth, V. K., and Pramod, R. (2021b). "Investigation on structural characteristics of bamboo-laminates," *IOP Conference Series: Materials Science and Engineering* 1185, article ID 12028. DOI: 10.1088/1757-899x/1185/1/012028
- Kurien, R. A., Selvaraj, D. P., Sekar, M., Koshy, C. P., Paul, C., Palanisamy, S., Santulli, C., and Kumar, P. (2023). "A comprehensive review on the mechanical, physical, and thermal properties of abaca fibre for their introduction into structural polymer composites," *Cellulose* 30, 1-22. DOI: 10.1007/s10570-023-05441-z
- LaDou, J. (2004). "The asbestos cancer epidemic," *Environmental Health Perspectives* 112(3), 285-290. DOI: 10.1289/ehp.6704
- Lv, Y., Wu, X., Gao, M., Chen, J., Zhu, Y., Cheng, Q., and Chen, Y. (2019). "Flexural behavior of basalt fiber reinforced polymer tube confined coconut fiber reinforced concrete," *Advances in Materials Science and Engineering* 2019, article ID 1670478. DOI: 10.1155/2019/1670478
- Ma, Q., Dong, F., Gan, X., and Zhou, T. (2021). "Effects of different interface conditions on energy absorption characteristics of Al/carbon fiber reinforced polymer hybrid structures for multiple loading conditions," *Polymer Composites* 42(6), 2838-2863. DOI: 10.1002/pc.26019
- Ma, Q., Wang, K., Gan, X., and Tian, Y. (2022). "Optimization design in perforated AL-CFRP hybrid tubes under axial quasi-static loading," *International Journal of Crashworthiness* 27(5), 1317-1336. DOI: 10.1080/13588265.2021.1926852

- Mache, A., Deb, A., and Gupta, N. (2020). "An experimental study on performance of jute-polyester composite tubes under axial and transverse impact loading," *Polymer Composites* 41(5), 1796-1812. DOI: 10.1002/pc.25498
- Mirzamohammadi, S., Eslami-Farsani, R., and Ebrahimnezhad-Khaljiri, H. (2022). "The characterization of the flexural and shear performances of laminated aluminum/jute-basalt fibers epoxy composites containing carbon nanotubes: As multi-scale hybrid structures," *Thin-Walled Structures* 179, article ID 109690. DOI: 10.1016/j.tws.2022.109690
- Mirzamohammadi, S., Eslami-Farsani, R., and Ebrahimnezhad-Khaljiri, H. (2023). "The effect of hybridizing natural fibers and adding montmorillonite nanoparticles on the impact and bending properties of eco-friendly metal/composite laminates," *Advanced Engineering Materials* 25(12), article ID 2201791. DOI: 10.1002/ADEM.202201791
- Mohd Bakhori, S. N., Hassan, M. Z., Mohd Bakhori, N., Jamaludin, K. R., Ramlie, F., Md Daud, M. Y., and Abdul Aziz, S. (2022). "Physical, mechanical and perforation resistance of natural-synthetic fiber interply laminate hybrid composites," *Polymers* 14(7), article 1322. DOI: 10.3390/polym14071322
- Padmanabhan, R. G., Karthikeyan, S., Parthasarathy, C., and Arockiam, A. J. (2022). "Crashworthiness test on hollow section structural (HSS) frame by metal fiber laminates with various geometrical shapes - Review," *AIP Conference Proceedings* 2520(1), article ID 030010. DOI: 10.1063/5.0105050
- Padmanabhan, R. G., Rajesh, S., Karthikeyan, S., Palanisamy, S., Ilyas, R. A., Ayrilmis, N., Tag-eldin, E. M., and Kchaou, M. (2024). "Evaluation of mechanical properties and Fick's diffusion behaviour of aluminum-DMEM reinforced with hemp/bamboo/basalt woven fiber metal laminates (WFML) under different stacking sequences," *Ain Shams Engineering Journal* 15(7), article ID 102759. DOI: 10.1016/j.asej.2024.102759
- Palaniappan, M., Palanisamy, S., Khan, R. H., Alrasheedi, N., Tadepalli, S., Murugesan, T., and Santulli, C. (2024). "Synthesis and suitability characterization of microcrystalline cellulose from Citrus x sinensis sweet orange peel fruit waste-based biomass for polymer composite applications," *Journal of Polymer Research* 31(4), article 105. DOI: 10.1007/s10965-024-03946-0
- Palanisamy, S., Kalimuthu, M., Azeez, A., Palaniappan, M., Dharmalingam, S., Nagarajan, R., and Santulli, C. (2022). "Wear properties and post-moisture absorption mechanical behavior of kenaf/banana-fiber-reinforced epoxy composites," *Fibers* 10(4), article 32. DOI: 10.3390/fib10040032
- Palanisamy, S., Kalimuthu, M., Dharmalingam, S., Alavudeen, A., Nagarajan, R., Ismail, S. O., Siengchin, S., Mohammad, F., and Al-Lohedan, H. A. (2023a). "Effects of fiber loadings and lengths on mechanical properties of *Sansevieria cylindrica* fiber reinforced natural rubber biocomposites," *Materials Research Express* 10(8), article ID 85503. DOI: 10.1088/2053-1591/acefb0
- Palanisamy, S., Kalimuthu, M., Santulli, C., Palaniappan, M., Nagarajan, R., and Fragassa, C. (2023b). "Tailoring epoxy composites with *Acacia caesia* bark fibers: Evaluating the effects of fiber amount and length on material characteristics," *Fibers* 11(7), article 63. DOI: 10.3390/fib11070063
- Persico, L., Giacalone, G., Cristalli, B., Tufano, C., Saccorotti, E., Casalone, P., and Mattiazzo, G. (2022). "Recycling process of a basalt fiber-epoxy laminate by solvolysis: Mechanical and optical tests," *Fibers* 10(6), article 55. DOI: 10.3390/fib10060055

- Prasath, K. A., Arumugaprabu, V., Amuthakkannan, P., Naresh, K., Muthugopal, M. S., Jeganathan, M., and Pragadeesh, R. (2020). "Quasi static and flexural mechanical property evaluation of basalt/flax reinforced composites," *Materials Physics and Mechanics* 46, 132-138. DOI: 10.18149/MPM.4612020\_13
- Rouzegar, J., Assaee, H., Elahi, S. M., and Asiaei, H. (2018). "Axial crushing of perforated metal and composite-metal tubes," *Journal of the Brazilian Society of Mechanical Sciences and Engineering* 40, 1-16. DOI: 10.1007/s40430-018-1266-6
- Sadoun, A. M., Abd El-Wadoud, F., Fathy, A., Kabeel, A. M., and Megahed, A. A. (2021). "Effect of through-the-thickness position of aluminum wire mesh on the mechanical properties of GFRP/Al hybrid composites," *Journal of Materials Research and Technology* 15, 500-510. DOI: 10.1016/j.jmrt.2021.08.026
- Sivagurunathan, R., Way, S. L. T., Sivagurunathan, L., and Yaakob, M. Y. (2018). "Effects of triggering mechanisms on the crashworthiness characteristics of square woven jute/epoxy composite tubes," *Journal of Reinforced Plastics and Composites* 37(12), 824-840. DOI: 10.1177/0731684418763218
- Sumesh, K. R., Ajithram, A., Palanisamy, S., and Kavimani, V. (2023). "Mechanical properties of ramie/flax hybrid natural fiber composites under different conditions," *Biomass Conversion and Biorefinery* 2023, 1-12. DOI: 10.1007/s13399-023-04628-5
- Stayner, L., Smith, R., Bailer, J., Gilbert, S., Steenland, K., Dement, J., Brown, D., & Lemen, R. (1996). Exposure-response analysis of risk of respiratory disease associated with occupational exposure to chrysotile asbestos. *Occupational and Environmental Medicine*, 53(12), 781-788. DOI: 10.1136/oem.53.12.781
- Supian, A. B. M., Sapuan, S. M., Zuhri, M. Y. M., Zainudin, E. S., and Ya, H. H. (2018). "Hybrid reinforced thermoset polymer composite in energy absorption tube application: A review," *Defence Technology* 14(4), 291-305. DOI: 10.1016/j.dt.2018.04.004
- Supian, A., Sapuan, S., Zuhri, M., Zainudin, E., and Ya, H. (2020). "Crashworthiness performance of hybrid kenaf/glass fiber reinforced epoxy tube on winding orientation effect under quasi-static compression load," *Defence Technology* 16(5), 1051-1061. DOI: 10.1016/j.dt.2019.11.012
- Vinod, A., Tengsuthiwat, J., Gowda, Y., Vijay, R., Sanjay, M. R., Siengchin, S., and Dhakal, H. N. (2022). "Jute/hemp bio-epoxy hybrid bio-composites: Influence of stacking sequence on adhesion of fiber-matrix," *International Journal of Adhesion and Adhesives* 113, article ID 103050. DOI: 10.1016/j.ijadhadh.2021.103050
- Yang, H., Lei, H., Lu, G., Zhang, Z., Li, X., and Liu, Y. (2020). "Energy absorption and failure pattern of hybrid composite tubes under quasi-static axial compression," *Composites Part B: Engineering* 198, article ID 108217. DOI: 10.1016/j.compositesb.2020.108217
- Zhang, Z., Sun, W., Zhao, Y., and Hou, S. (2018). "Crashworthiness of different composite tubes by experiments and simulations," *Composites Part B: Engineering* 143, 86-95. DOI: 10.1016/j.compositesb.2018.01.021
- Zhu, G., Zhao, X., Shi, P., and Yu, Q. (2019). "Crashworthiness analysis and design of metal/CFRP hybrid structures under lateral loading," *IEEE Access* 7, 64558-64570. DOI: 10.1109/ACCESS.2019.2917284

Article submitted: May 25, 2024; Peer review completed: July 19, 2024; Revisions accepted: July 23, 2024; Published: July 26, 2024.  
DOI: 10.15376/biores.19.3.6584-6604